MNRAS **454,** 1503–1508 (2015) doi:10.1093/mnras/stv2008

A model of plasma heating by large-scale flow

P. Pongkitiwanichakul,[1⋆] F. Cattaneo,[1] S. Boldyrev,[2,3] J. Mason[4] and J. C. Perez[5,6]

[1]*Department of Astronomy and Astrophysics, University of Chicago, Chicago, IL 60637, USA*
[2]*Department of Physics, University of Wisconsin at Madison, WI 53706, USA*
[3]*Space Science Institute, Boulder, CO 80301, USA*
[4]*College of Engineering, Mathematics and Physical Sciences, University of Exeter, Exeter EX4 4QF, UK*
[5]*Space Science Center, University of New Hampshire, Durham, NH 03824, USA*
[6]*Department of Physics and Space Sciences, Florida Institute of Technology, Melbourne, FL 32901, USA*

Accepted 2015 August 27. Received 2015 August 21; in original form 2015 May 12

ABSTRACT

In this work, we study the process of energy dissipation triggered by a slow large-scale motion of a magnetized conducting fluid. Our consideration is motivated by the problem of heating the solar corona, which is believed to be governed by fast reconnection events set off by the slow motion of magnetic field lines anchored in the photospheric plasma. To elucidate the physics governing the disruption of the imposed laminar motion and the energy transfer to small scales, we propose a simplified model where the large-scale motion of magnetic field lines is prescribed not at the footpoints but rather imposed volumetrically. As a result, the problem can be treated numerically with an efficient, highly accurate spectral method, allowing us to use a resolution and statistical ensemble exceeding those of the previous work. We find that, even though the large-scale deformations are slow, they eventually lead to reconnection events that drive a turbulent state at smaller scales. The small-scale turbulence displays many of the universal features of field-guided magnetohydrodynamic turbulence like a well-developed inertial range spectrum. Based on these observations, we construct a phenomenological model that gives the scalings of the amplitude of the fluctuations and the energy-dissipation rate as functions of the input parameters. We find good agreement between the numerical results and the predictions of the model.

Key words: magnetic fields – MHD – plasmas – turbulence – waves – Sun: corona.

1 INTRODUCTION

The mechanism by which energy is extracted from large-scale plasma flows and converted into heat is one of the fundamental problems in astrophysical magnetohydrodynamics. The energy may be dissipated in large current and vorticity sheets, transferred to small scales via a turbulent cascade, converted into heat in a very large number of tiny current sheets, or dissipated in a fashion incorporating several of these mechanisms. One of the applications of the theory is the problem of particle heating and acceleration in the solar corona that is hundreds of times hotter than the solar photosphere (Aschwanden 2004; Klimchuk 2006). The most accepted mechanism involves converting coronal magnetic energy into heat. The magnetic field is assumed to be frozen into the plasma, so that the twisting and tangling of magnetic field lines by the photospheric footpoint motions eventually releases magnetic energy in the process of magnetic reconnection (Yamada, Kulsrud & Ji 2010).

In this study, we are interested in the case of a slow large-scale motion of the magnetic field lines, i.e. slow compared to the time-scale for the Alfvén waves to propagate back and forth along the field lines through the system. This corresponds to the case of slow footpoint motion in coronal heating, where the magnetic loops respond by evolving slowly through a sequence of magnetostatic equilibria (Gold & Hoyle 1960; Barnes & Sturrock 1972; van Ballegooijen 1986). As not all of the equilibria have the same magnetic topology, the deformation of an equilibrium with one topology into another happens through the process of magnetic reconnection, which converts magnetic energy into kinetic energy of the plasma particles (e.g. Parker 1972; Ng & Bhattacharjee 1998; Priest & Forbes 2000; Low 2015).

This process is often studied in the framework of the Parker model (Parker 1972, 1988), where the coronal loops are treated as straight plasma columns. The initially uniform magnetic field lines in a column are attached at both ends to the perfectly conducting boundaries where the slow plasma motion is prescribed. The problem cannot be solved analytically in its most general form and the available numerical simulations can only address Reynolds numbers that are hopelessly below the astrophysically relevant values. Consequently, the goal of phenomenological and numerical treatments is to establish the plasma heating rate and, in particular, its scaling with the magnetic Reynolds number Rm, in the hope that

⋆ E-mail: peera@uchicago.edu

the results may be extrapolated to the naturally relevant parameter regimes (e.g. Longcope & Sudan 1994; Rappazzo & Velli 2011; Ng, Lin & Bhattacharjee 2012; Wan et al. 2014).

In the phenomenological treatment proposed in Longcope & Sudan (1994), it was assumed that in the limit of large Rm the energy dissipation occurs in a finite number of isolated Sweet–Parker current sheets. The heating rate was then predicted to scale as $\epsilon \propto Rm^{1/3}$. In more recent studies by Ng & Bhattacharjee (2008) and Ng et al. (2012) it was proposed that the scaling essentially depends on the rate of magnetic field 'stirring' by the footpoint motion. If the typical time of the field line twisting by random footpoint motion is smaller than the typical time of the magnetic energy build-up and release cycle, then the heating rate becomes independent of the Reynolds number. This conclusion was supported in part by numerical simulations at moderate Rm.

In this work, we propose that in the limit of large Reynolds numbers, the fast random magnetic line twisting and tangling does not need to be imposed by footpoint motion. Rather, it is naturally provided by the small-scale turbulence that inevitably develops in such a regime. Once the turbulence is developed, the rate of energy dissipation is dictated by the rate of energy cascade towards small scales, which is independent of the Reynolds number. This picture therefore does not require the random rapid motion of the footpoints. Moreover, it does not require the assumption of a finite number of current sheets in the limit of large Rm. Such an assumption would in fact be incorrect, as the number of current sheets responsible for energy dissipation in magnetohydrodynamic (MHD) turbulence is known to increase as the Reynolds number increases (e.g. Zhdankin et al. 2013).

To support our phenomenological theory with numerical simulations, we propose a so-called volumetric Parker model, where instead of prescribing the displacements of the footpoints, we impose a slow large-scale velocity throughout the entire volume of the fluid. The justification for this modification is that for high Alfvén velocities a boundary displacement is communicated almost instantaneously along the field lines. A practical advantage of our model is that the volumetric displacement problem can be embedded in a three-dimensional (3D) periodic domain and treated numerically with an efficient, highly accurate spectral method. This allows us to study the problem with a resolution and statistical ensemble exceeding those of previous studies, and to derive novel scaling laws for the dependence of the magnetic and kinetic fluctuations on the parameters of the large-scale flow.

2 MODEL

We solve the full 3D incompressible dissipative MHD equations[1] with an additional volumetric forcing term,

$$\frac{\partial}{\partial t}\boldsymbol{v} + \boldsymbol{v}\cdot\nabla\boldsymbol{v} - \boldsymbol{b}\cdot\nabla\boldsymbol{b} - \hat{\boldsymbol{v}}_A\cdot\nabla\boldsymbol{b} = -\nabla P + S^{-1}\nabla^2\boldsymbol{v} + \boldsymbol{F}, \quad (1)$$

$$\frac{\partial}{\partial t}\boldsymbol{b} + \boldsymbol{v}\cdot\nabla\boldsymbol{b} - \boldsymbol{b}\cdot\nabla\boldsymbol{v} - \hat{\boldsymbol{v}}_A\cdot\nabla\boldsymbol{v} = S^{-1}\nabla^2\boldsymbol{b}, \quad (2)$$

$$\nabla\cdot\boldsymbol{v} = 0, \quad \nabla\cdot\boldsymbol{b} = 0, \quad (3)$$

where $\boldsymbol{v}_A = \boldsymbol{B}_0/\sqrt{4\pi\rho_0}$ is the Alfvén velocity based upon the uniform background magnetic field $\boldsymbol{B}_0$ which is in the z-direction, $\boldsymbol{v}$ is the fluctuating plasma velocity normalized by v_A, $\boldsymbol{b}$ is the fluctuating magnetic field normalized by v_A, $P = (p + b^2/2)$, p is the plasma pressure normalized to $\rho_0 v_A^2$, ρ_0 is the background plasma density, $S = v_A L_\perp/\nu$ is the (constant) Lundquist number (the magnetic Prandtl number Pm is set to unity, that is, fluid viscosity is equal to magnetic diffusivity), $L_\perp$ is a characteristic scale length transverse to $\boldsymbol{B}_0$ and $\boldsymbol{F}$ is a forcing term. In these equations time is normalized by the Alfvén time $L_\perp/v_A$ and spatial coordinates are normalized by $L_\perp$.

The driving of the system is performed by ensuring that the large-scale velocity field $\boldsymbol{v}_0$, say, that occupies certain wavenumbers (see below), is time independent, while the remaining Fourier components of the velocity field are allowed to evolve. The prescribed part of the velocity field is defined by

$$\boldsymbol{v}_0 = \hat{\boldsymbol{z}}\times\nabla\psi, \quad (4)$$

where

$$\psi = v_0 L_\perp \sin(z/L_\parallel)\left[\cos(x/L_\perp) + \cos(y/L_\perp)\right] - (v_0 L_\perp/2)\cos(z/L_\parallel)\left[\cos(2x/L_\perp) + \cos(2y/L_\perp)\right]. \quad (5)$$

Thus, at each time step, the Fourier components of $\boldsymbol{v}_0$ are kept fixed while the remaining components of the velocity are allowed to vary.

An equivalent way of looking at this driving mechanism is to assume that all of the components of the velocity field are allowed to evolve, but the large-scale force $\boldsymbol{F}$ in equation (1) is chosen in such a way that at each time step it brings the large-scale component of the velocity field back to its prescribed value (5). This is the interpretation that we will use in what follows.

It is important to stress that the imposed weak velocity field v_0 is not strong enough to drive turbulence in the absence of the magnetic field. Its detailed form is not important, however, it should be chosen so that it will engender non-trivial deformations of the magnetic field. Here, we have chosen a flow with a simple, large-scale cellular structure and non-trivial trajectories. The dynamics of the system thus essentially depends on the build-up and release of magnetic energy, which we discuss in detail in the next sections.

We also note that we do not aim at providing a detailed explanation of coronal heating. Rather, we concentrate on a fundamental mechanism of energy extraction from large-scale MHD flows. We however believe that in the parameter regime $(v_A L_\perp)/(v_0 L_\parallel) \gg 1$, our approach should be qualitatively similar other approaches based on line-tying.[2]

The numerical code solves equations (1–3) in a triply periodic rectangular domain of cross-sectional area $(2\pi L_\perp)^2$ and height $2\pi L_\parallel$, where the subscripts denote the directions perpendicular and parallel to the background magnetic field. We use a fully dealiased 3D pseudo-spectral algorithm to perform the spatial discretization on a grid with a resolution of 512^3 mesh points. A description of the numerical scheme may be found in Cattaneo, Emonet & Weiss (2003).

3 RESULTS

In the following sections, we present the results of a series of simulations. The parameters of the simulations are summarized in Table 1. The values of the Lundquist number S, which is kept constant in

[1] We note that in studies of MHD turbulence with a strong guide field, the reduced MHD approximation is often used. We do not make such an approximation in our analysis.

[2] We do not make such an approximation here.

Table 1. Summary of the simulation parameters. Here, T denotes the total physical time for each simulation.

Run no.	$L_\parallel/L_\perp$	v_0/v_A	S	$v_\mathrm{A}T/L_\perp$
A1	1	1.25×10^{-3}	8000	1.2×10^4
A2	1	2.5×10^{-3}	4000	5.8×10^3
A3	1	5×10^{-3}	4000	3.2×10^3
A41	1	1×10^{-2}	1000	5.4×10^3
A42	1	1×10^{-2}	2000	5.4×10^3
A43	1	1×10^{-2}	4000	4.4×10^3
A44	1	1×10^{-2}	8000	4.9×10^3
A5	1	2×10^{-2}	4000	1.8×10^3
A6	1	4×10^{-2}	4000	1.2×10^3
B1	3	1.25×10^{-3}	32 000	2.0×10^4
B2	3	2.5×10^{-3}	16 000	1.6×10^4
B3	3	5×10^{-3}	8000	2.0×10^4
B41	3	1×10^{-2}	5000	6.0×10^3
B42	3	1×10^{-2}	8000	8.4×10^3
B43	3	1×10^{-2}	12 500	8.7×10^3
B5	3	2×10^{-2}	8000	5.7×10^3
B6	3	4×10^{-2}	8000	1.8×10^3
C1	8	1.5×10^{-3}	32 000	9.6×10^3
C2	8	3.3×10^{-3}	32 000	2.0×10^4
C3	8	2×10^{-2}	8000	9.6×10^3

each simulation, are limited from above by the requirement that the resulting turbulent fluctuations are well resolved at the grid scale. By well resolved we mean that the high wavenumber tail of the spectra has a fast falloff. The values of the Lundquist number S are limited from below by the requirement that the magnetic Reynolds number based on the prescribed flow v_0, $Rm_0 = (v_0/v_A)S$ exceeds unity so that the magnetic field lines can be advected by the flow. The Reynolds numbers of the fluctuations (which are not known in advance) are calculated after both the velocity and magnetic fields reach statistically steady states. In some cases, multiple values of S are used to establish the scaling with the Lundquist number. The last column shows the time duration T of each simulation normalized to $L_\perp/v_A$. We also note that larger values of $L_\parallel v_A/(L_\perp v_0)$ typically mean that a larger computational time is required. The ratio v_0/v_A is quite small in our simulations, which is also the case in the solar corona.

Cyclic bursts. First, we focus on the time evolution of the kinetic and magnetic energies, v^2 and b^2, and the energy-dissipation rate, ϵ.[3] We do not separate viscous and ohmic heating as they are similar to each other. As an illustrative example, Fig. 1 shows v^2, b^2 and ϵ from run B42. The energies and the heating rate are highly intermittent but they are related to each other. At first, the prescribed flow $\boldsymbol{v}_0$ disturbs the large scale field $\boldsymbol{B}_0$ and the magnetic perturbation $\boldsymbol{b}_0$ is generated. The Fourier modes of $\boldsymbol{b}_0$ are the same as the modes of $\boldsymbol{v}_0$. This process increases the magnetic energy until the term $\boldsymbol{b}_0 \cdot \nabla \boldsymbol{b}_0$ generates the velocity fluctuations $\delta\boldsymbol{v}$ with higher harmonics than those in $\boldsymbol{v}_0$. The total velocity field is then $\boldsymbol{v} = \boldsymbol{v}_0 + \delta\boldsymbol{v}$.

Eventually, the velocity and magnetic perturbations are developed at scales small enough to cause the release of the magnetic energy accumulated in $\boldsymbol{b}_0$ by non-ideal processes. This happens in a short time-scale in the form of a burst that transfers magnetic energy into plasma flow and heat. This may be consistent

[3] We identify the dissipation rate with the heating rate ϵ, which is an appropriate association to make in incompressible MHD as it does not model plasma heating directly.

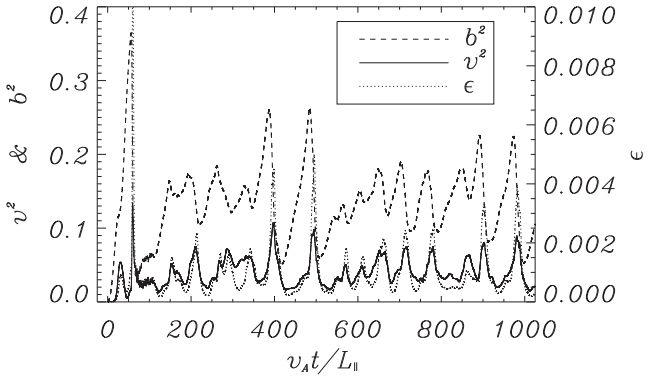

Figure 1. The time series of ϵ, v^2 and b^2 from simulation B42.

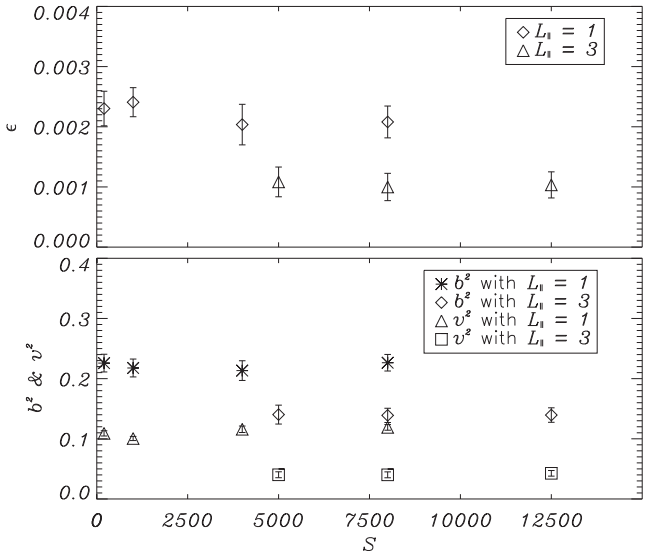

Figure 2. The time-averaged values of ϵ (upper panel) and of b^2 and v^2 (lower panel) from simulations A41–44 and B41–43.

with a fast and intermittent rearrangement of magnetic field lines and energy release due to magnetic reconnection (e.g. Rappazzo et al. 2008; Fuentes-Fernández, Parnell & Priest 2012; Osman et al. 2012; Huang, Bhattacharjee & Boozer 2014; Higashimori, Yokoi & Hoshino 2013; Leonardis et al. 2013). After the energy of $\boldsymbol{b}_0$ has been released, there is no energy to feed $\delta\boldsymbol{v}$. Both $\boldsymbol{b}_0$ and $\delta\boldsymbol{v}$ then decrease. The energy in $\boldsymbol{b}_0$ is then reaccumulated by $\boldsymbol{v}_0$ and the process repeats itself. This cyclic process is responsible for the intermittency observed in v^2, b^2 and ϵ. It is reasonable to assume that the solution is self-correlated during only one cycle, therefore, the cycle period τ_c also plays the role of the correlation time of the fluctuations in the system.

Scaling with Lundquist number. To study how v^2, b^2 and ϵ depend on the Lundquist number S, we compare the results from simulations A41–44 and B41–43. The time-averaged dissipation rate ϵ, as well as the fluctuation energies, b^2 and v^2, from these simulations are shown in Fig. 2. They appear to be independent of S. Since the values of Re are proportional to S, we can also claim that ϵ, b^2 and v^2 are independent of the Reynolds number.

An important feature of our $Pm = 1$ simulations is that both viscous and ohmic heating are very similar. This is consistent with the presence of small-scale turbulence governing the energy

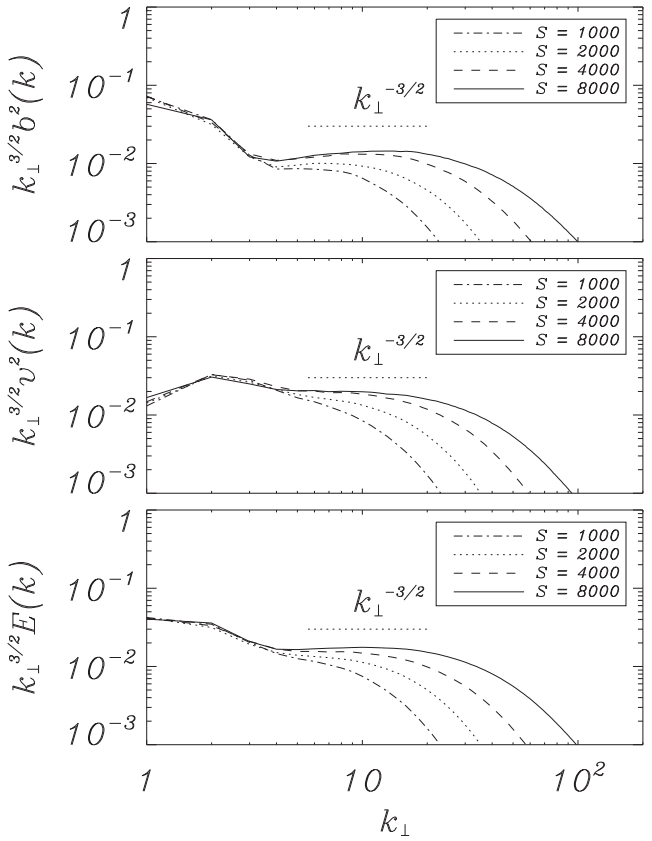

Figure 3. The time averaged power spectra of b^2 (upper panel), v^2 (middle panel), and $E = 0.5(v^2 + b^2)$ (lower panel) from simulations A41–44.

cascade and energy dissipation in the system. Indeed, the values of the time-averaged *Re* range from 300 to 2700, so turbulence may develop. To verify this scenario, we plot the energy power spectra obtained in simulations A41–44, in Fig. 3. Beyond the transitional range of scales observed at $k_\perp \leq 3$, both magnetic and velocity fluctuations exhibit broad energy spectra with the spectral indices approaching $-3/2$ as S increases. We believe that this is a signature of MHD turbulence developing in the system (e.g. Müller & Grappin 2005; Perez et al. 2012; Tobias, Cattaneo & Boldyrev 2013), which is responsible for removing the energy from the large scale and transferring it into heat with the rate independent of the Reynolds and Lundquist numbers.

Scaling with the large-scale parameters. In this section, we relate the energies of the fluctuations v^2 and b^2, and the dissipation rate ϵ to the large-scale parameters of the system, B_0, v_0, $L_\parallel$ and $L_\perp$. In steady-state turbulence, the rate of energy dissipation at small scales is equal to the rate of energy cascade over scales and to the rate of energy supply at large scales. The driving force in equations (1–3) is needed to keep the large-scale velocity field $\boldsymbol{v}_0$ prescribed, therefore, it should balance the large-scale magnetic force, estimated as $(\boldsymbol{v}_A \cdot \nabla)\boldsymbol{b}_0$. Recall that the magnetic fluctuations $\boldsymbol{b}_0$ result from a shuffling of the uniform magnetic field $\boldsymbol{B}_0$ by the large-scale flow $\boldsymbol{v}_0$, and that $\boldsymbol{b}_0$ has the same set of Fourier modes as $\boldsymbol{v}_0$. The energy input rate per unit volume is therefore estimated as

$$\epsilon \sim \langle \boldsymbol{v}_0 \cdot \boldsymbol{F} \rangle \sim -\langle \boldsymbol{v}_0 \cdot (\boldsymbol{v}_A \cdot \nabla)\boldsymbol{b}_0 \rangle \sim v_A v_0 b_0 / L_\parallel, \quad (6)$$

where $L_\parallel$ is the typical field-parallel scale of $\boldsymbol{v}_0$. This rate should coincide with the rate of energy transfer to small scales in the turbulent cascade,

$$\epsilon \sim \langle \delta\boldsymbol{v} \cdot (\delta\boldsymbol{b} \cdot \nabla_\perp)\delta\boldsymbol{b} \rangle \sim \delta v^3 / l_\perp, \quad (7)$$

where $\delta v \sim \delta b$ are the turbulent fluctuations at the outer scale of turbulence, $l_\perp$ (this scale approximately corresponds to $k_\perp = 3$ in Fig. 3). Here the magnetic fluctuations $\delta\boldsymbol{b}$ have Fourier harmonics with $k \geq 3$.

In a steady state, there is a balance between generation of the large-scale magnetic fluctuations $\boldsymbol{b}_0$, and their diffusion due to small-scale turbulence. The generation of magnetic fluctuations by the large-scale flow $\boldsymbol{v}_0$ is given by the term $(\boldsymbol{v}_A \cdot \nabla)\boldsymbol{v}_0$ with the magnitude $\sim v_A v_0 / L_\parallel$ in the induction equation, while their diffusion due to turbulence is described by $\eta_T b_0 / L_\perp^2 \sim l_\perp \delta v b_0 / L_\perp^2$, where we have substituted $\eta_T \sim l_\perp \delta v$ for the turbulent diffusivity and $L_\perp$ is the typical field-perpendicular scale of $\boldsymbol{v}_0$. We thus arrive at the balance condition

$$v_A v_0 / L_\parallel \sim l_\perp \delta v b_0 / L_\perp^2. \quad (8)$$

From (6), (7) and (8) we obtain the amplitudes of the turbulent fluctuations

$$\delta v^2 \sim \delta b^2 \sim v_0 v_A L_\perp / L_\parallel, \quad (9)$$

and the energy-dissipation rate per unit mass

$$\epsilon \sim (v_0 v_A L_\perp / L_\parallel)^{3/2} l_\perp^{-1}. \quad (10)$$

Fig. 4 shows how δb^2, δv^2 and ϵ depend on $v_0/L_\parallel$ in all of the simulations. They are in good agreement with our phenomenological estimates. We also note that from equations (6), (7) and (8) one derives $(\delta b / b_0)^2 \sim (l_\perp / L_\perp)^2$, which is consistent with Fig. 3.

Finally, we are in a position to estimate the large-scale correlation time τ_c. Since large-scale magnetic fluctuations grow up to b_0 on the correlation time-scale, from the induction equation we obtain $b_0/\tau_c \sim v_A v_0 / L_\parallel$. Substituting for $b_0 \sim (L_\perp / l_\perp)\delta b$, and using result (9), we estimate the correlation time

$$\tau_c \sim (L_\parallel / v_A)^{1/2} (L_\perp / v_0)^{1/2} (L_\perp / l_\perp). \quad (11)$$

According to our previous discussion, this time also characterizes the burst cycles of the large-scale fluctuations.

4 DISCUSSION AND CONCLUSION

We have presented a numerical and phenomenological study of the coronal heating problem based on the so-called volumetric Parker model. In this model the slow large-scale motion of the magnetic field lines is prescribed not at the boundaries of the domain, but throughout the volume of the fluid. As a result, the model allows for an effective numerical study, with the resolution, statistical ensemble and accuracy exceeding those of previous treatments.

We have established that energy is extracted from the prescribed slow flow in a bursty, intermittent fashion. Energy is quickly redistributed over large scales and transferred to small dissipative scales (large $k_\perp$ modes) through a universal turbulent cascade. The energy-dissipation rate and the levels of the magnetic and velocity fluctuations are independent of the magnetic Reynolds and Lundquist numbers. However, there is a dependence on the large-scale parameters of the prescribed flow, with the scaling given by equations (9) and (10).

To give a sense of magnitudes and scales, we make order of magnitude estimates based on equation (10). If a proton–electron plasma is assumed, then equation (10) can be used to estimate the

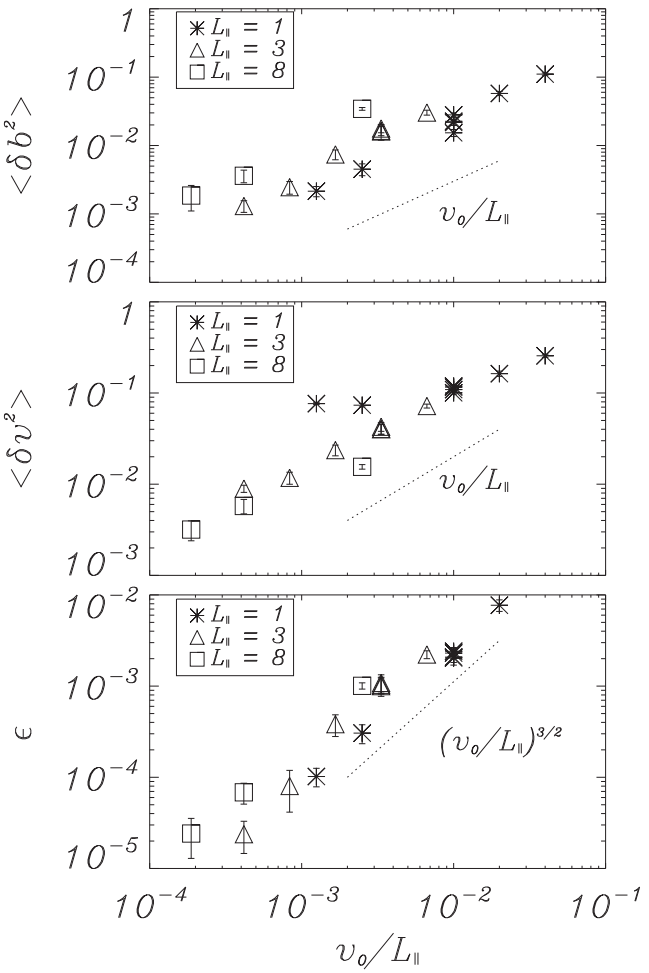

Figure 4. The time averaged δb^2 at $k \geq 3$, δv^2 and ϵ from all simulations versus $v_0/L_\parallel$. (The slight upshift of the magnetic fluctuations, denoted by squares in the upper panel, may be related to our somewhat subjective separation of the stronger large-scale component b_0 from the weaker turbulent component δb at $k = 3$. No upshift is observed in the corresponding velocity fluctuations that do not develop a strong large-scale component.)

energy-dissipation rate per unit volume:

$$E_{\rm diss} = \epsilon\rho = 5.3 \times 10^{-3} \left(\frac{v_0}{10^5\ {\rm cm\,s^{-1}}}\right)^{3/2} \left(\frac{v_{\rm A}}{10^8\ {\rm cm\,s^{-1}}}\right)^{3/2} \times \left(\frac{n_0}{10^9 {\rm cm^{-3}}}\right) \left(\frac{L_\perp}{L_\parallel}\right)^{3/2} \left(\frac{l_\perp}{10^7 cm}\right)^{-1} {\rm erg\,s^{-1} cm^{-3}}, \quad (12)$$

where n_0 is the number of protons or electrons, and ρ is the mass density. If we assume $v_0 = 5 \times 10^5$ cm s^{-1}, $v_{\rm A} = 2 \times 10^8$ cm s^{-1}, $n_0 = 2.5 \times 10^9$ cm^{-3}, $L_\perp = 10^8$ cm, $L_\parallel = 4 \times 10^9$ cm and $l_\perp = L_\perp/2$, the dissipation rate becomes $E_{\rm diss} = 3.33 \times 10^{-4}$ erg s^{-1} cm^{-3}. This rate is equivalent to having the energy flux $E_{\rm diss} L_\parallel = 1.32 \times 10^6$ erg s^{-1} cm^{-2} through the boundaries with an area of $L_\perp^2$. This energy flux is within order of magnitude agreement with the required flux to heat the corona (cf. Aschwanden 2004; De Pontieu et al. 2007, 2011; McIntosh et al. 2011). This estimate for the energy flux is not unreasonble given the idealized nature of our model. For an extensive review of the most recent advances in understanding the coronal heating problem and the acceleration of the solar wind, the reader is referred to De Moortel & Browning (2015).

Our treatment is different and complementary to the previous studies where the role of imposed random tangling of magnetic field lines and magnetic turbulence in the energy dissipation was also discussed (e.g. Dmitruk, Gómez & DeLuca 1998; Dmitruk & Gómez 1999; Rappazzo et al. 2008; Ng et al. 2012). In those studies, the magnetic field columns were distorted at the boundaries rather than volumetrically, which mathematically imposed perturbations with a broad spectrum of field-parallel wavenumbers $k_\parallel$. In our case, the driving is strictly confined to the large-scale modes so that the small-scale dissipation cannot be affected by the driving directly. The observed spectrum and scaling of the fluctuations is solely a consequence of the non-linear dynamics. In addition, in contrast with Ng et al. (2012), we observed an S-independent dissipation rate without imposing an external fast field-line shuffling. In contrast with Rappazzo et al. (2008), we use the full MHD treatment (rather than RMHD) as we do not make a priori assumptions about the nature of turbulence that may develop in the system (e.g. the relevance of field-parallel fluctuations, transport of field-parallel momentum, etc., which are all neglected in RMHD). Finally, in contrast with Dmitruk et al. (1998) and Dmitruk & Gómez (1999) where the 2D MHD equations were used, we use a full 3D treatment and our analytically and numerically derived scaling of the fluctuating fields [equation (9)] is different from their predictions.

ACKNOWLEDGEMENTS

This research was supported by the NSF Center for Magnetic Self-Organization in Laboratory and Astrophysical Plasmas at the University of Chicago, by the US DOE award no. DE-SC0003888, by the NASA grant no. NNX11AE12G, and by the National Science Foundation under grant no. NSF PHY11-25915 and no. AGS-1261659. SB and JM appreciate the hospitality and support of the Kavli Institute for Theoretical Physics, University of California, Santa Barbara, where part of this work was conducted. Simulations were performed at the Texas Advanced Computing Center (TACC) at the University of Texas at Austin under the NSF-Teragrid Projects TG-AST140015 & TG-PHY120042 and by the National Institute for Computational Sciences.

REFERENCES

Aschwanden M. J., 2004, Physics of the Solar Corona: an Introduction with Problems and Solutions. Springer-Verlag, Berlin
Barnes C. W., Sturrock P. A., 1972, ApJ, 174, 659
Cattaneo F., Emonet T., Weiss N., 2003, ApJ, 588, 1183
De Moortel I., Browning P., 2015, Phil. Trans. R. Soc. A, 373, 40269
De Pontieu B. et al., 2007, Science, 318, 1574
De Pontieu B. et al., 2011, Science, 331, 55
Dmitruk P., Gómez D. O., 1999, ApJ, 527, L63
Dmitruk P., Gómez D. O., DeLuca E. E., 1998, ApJ, 505, 974
Fuentes-Fernández J., Parnell C. E., Priest E. R., 2012, Phys. Plasmas, 19, 072901
Gold T., Hoyle F., 1960, MNRAS, 120, 89
Higashimori K., Yokoi N., Hoshino M., 2013, Phys. Rev. Lett., 110, 255001
Huang Y.-M., Bhattacharjee A., Boozer A. H., 2014, ApJ, 793, 106
Klimchuk J., 2006, Sol. Phys., 234, 41
Leonardis E., Chapman S. C., Daughton W., Roytershteyn V., Karimabadi H., 2013, Phys. Rev. Lett., 110, 205002
Longcope D. W., Sudan R. N., 1994, ApJ, 437, 491
Low B. C., 2015, Sci. China Phys. Mech. Astron., 58, 2
McIntosh S. W., de Pontieu B., Carlsson M., Hansteen V., Boerner P., Goossens M., 2011, Nature, 475, 477
Müller W., Grappin R., 2005, Phys. Rev. Lett., 95, 114502
Ng C. S., Bhattacharjee A., 1998, Phys. Plasmas, 5, 4028

Ng C. S., Bhattacharjee A., 2008, ApJ, 675, 899
Ng C. S., Lin L., Bhattacharjee A., 2012, ApJ, 747, 109
Osman K. T., Matthaeus W. H., Wan M., Rappazzo A. F., 2012, Phys. Rev. Lett., 108, 261102
Parker E. N., 1972, ApJ, 174, 499
Parker E. N., 1988, ApJ, 330, 474
Perez J. C., Mason J., Boldyrev S., Cattaneo F., 2012, Phys. Rev. X, 2, 041005
edsPriest E., Forbes T. 2000, Magnetic Reconnection : MHD Theory and Applications. Cambridge Univ. Press, Cambridge
Rappazzo A. F., Velli M., 2011, Phys. Rev. E, 83, 065401
Rappazzo A. F., Velli M., Einaudi G., Dahlburg R. B., 2008, ApJ, 677, 1348
Tobias S. M., Cattaneo F., Boldyrev S., 2013, in Davidson P. A., Kaneda Y., Sreenivasan K. R., eds, Ten Chapters in Turbulence. Cambridge Univ. Press, Cambridge, p. 351
van Ballegooijen A. A., 1986, ApJ, 311, 1001
Wan M., Rappazzo A. F., Matthaeus W. H., Servidio S., Oughton S., 2014, ApJ, 797, 63
Yamada M., Kulsrud R., Ji H., 2010, Rev. Mod. Phys., 82, 603
Zhdankin V., Uzdensky D. A., Perez J. C., Boldyrev S., 2013, ApJ, 771, 124

This paper has been typeset from a TEX/LATEX file prepared by the author.